ELSEVIER

Journal of Electron Spectroscopy and Related Phenomena 112 (2000) 221–230

JOURNAL OF ELECTRON SPECTROSCOPY and Related Phenomena

www.elsevier.nl/locate/elspec

Femtosecond stimulated emission pumping: Dynamics of vibrational energy loss in excited $I_2^-(CO_2)_4$ clusters

Alison V. Davis, Martin T. Zanni, Christian Frischkorn, Mohammed Elhanine[1], Daniel M. Neumark*

Department of Chemistry, University of California and Chemical Sciences Division, Laurence Berkeley National Laboratory, Berkeley, CA 94720, USA

Received 28 March 2000; accepted 6 June 2000

Abstract

Femtosecond stimulated emission pumping in conjunction with femtosecond photoelectron spectroscopy is used to monitor dynamics within $I_2^-(CO_2)_4$ following coherent vibrational excitation of the I_2^- chromophore. Femtosecond pump and dump pulses create an I_2^- wavepacket with 0.53 eV vibrational energy. Subsequent evolution of this wavepacket is monitored via its time-dependent photoelectron spectrum. At this energy, the vibrational frequency of the embedded I_2^- is 80 cm^{-1}, 7 cm^{-1} higher than that of bare I_2^-. As the I_2^- loses energy to the CO_2 molecules, the wavepacket frequency increases linearly at a rate of 3.8 cm^{-1}/ps during the initial 3 ps of coherence. The rate of energy transfer can be determined either by this increase in vibrational frequency or by the shift of the measured photoelectron spectrum. No solvent evaporation during the first 7 ps is observed, but three CO_2 molecules evaporate on a microsecond time scale.

Keywords: Photoelectron spectroscopy; Femtosecond lasers; Stimulated emission pumping; Anion clusters

1. Introduction

The transfer of vibrational energy from a solute to surrounding solvent molecules is a process of fundamental importance that has been investigated for many systems with a variety of techniques [1]. I_2^- has become a model system for ultrafast studies of vibrational energy transfer in a variety of polar solvents [2–4] and size-selected clusters [5–12], due both to the ease of size-selection for cluster studies and to its strong interaction with dipolar and polar solvent molecules. When I_2^- is photodissociated in these media, caging of the I and I^- fragments occurs, followed by recombination and vibrational relaxation. Experiments by Lineberger et al. [5–9], Barbara et al. [2–4], and our group [10–12] have probed these aspects of the dynamics, while molecular dynamics simulations have been performed by Parson et al. [13–16] and Coker et al. [17,18]. One problem in interpreting the experiments is that by the time that the signal from the recombined I_2^- is evident, significant vibrational relaxation has already occurred and the internal energy of the I_2^- is not known a priori. In this paper we describe an experi-

*Corresponding author. Tel.: +1-510-642-3502; fax: +1-510-642-6262.

E-mail address: dan@radon.cchem.berkeley.edu (D. Neumark).

[1]Present address: Laboratoire de Photophysique Moléculaire du CNRS, Bâtiment 210, Université Paris Sud, 91405 Orsay, France.

0368-2048/00/$ – see front matter
PII: S0368-2048(00)00215-2

ment in which the I_2^- moiety within the $I_2^-(CO_2)_4$ cluster is coherently excited with a known amount of vibrational energy using femtosecond stimulated emission pumping, and the resulting dynamics are followed by femtosecond photoelectron spectroscopy. This experiment probes not only the dynamics of a well-defined wavepacket within a size-selected cluster, but also how the I_2^- potential is modified by clustering.

SEP–FPES was recently demonstrated on bare I_2^- [19], where it was used to characterize the potential energy function of the $\tilde{X}^2\Sigma_u^+$ ground state up to energies very near the dissociation threshold. The overall experimental scheme for $I_2^-(CO_2)_4$ is very similar and is shown in Fig. 1, along with the calculated structure for this cluster [20]. The I_2^- moiety is excited from its ground $\tilde{X}^2\Sigma_u^+$ state to the repulsive $\tilde{A}'\ ^2\Pi_{g,1/2}$ state with a 795-nm femtosecond pump pulse. After a brief delay Δt_1, a femtosecond dump pulse projects a portion of the evolving wavepacket back down to the $\tilde{X}$ state, creating a coherent vibrational wavepacket which oscillates in the potential with a frequency characteristic of the potential and of its degree of excitation. The wavepacket dynamics are monitored by photodetachment with a femtosecond probe pulse and measurement of the resulting photoelectron spectrum.

In the case of bare I_2^-, the electron signal at particular electron kinetic energies shows oscillations corresponding to vibrational motion of the wavepacket. The wavepacket dephases after several ps due to the anharmonicity of the potential, but rephases at a much later time also determined by the anharmonicity. In $I_2^-(CO_2)_4$, several additional effects can occur due to interactions with the solvent molecules. First, the effective I_2^- potential may differ from that in bare I_2^-, resulting in a different wavepacket vibrational frequency at short observation times. Secondly, the vibrating I_2^- chromophore can lose energy to the surrounding solvent network, so that the ''SEP wavepacket'' slides down the potential as shown schematically in Fig. 1. This can result in a time-dependent oscillation frequency as well as overall changes in the appearance of the photoelectron spectrum. Finally, phase-changing collisions with the solvent molecules can result in different dephasing times than were seen in the bare I_2^-. All of

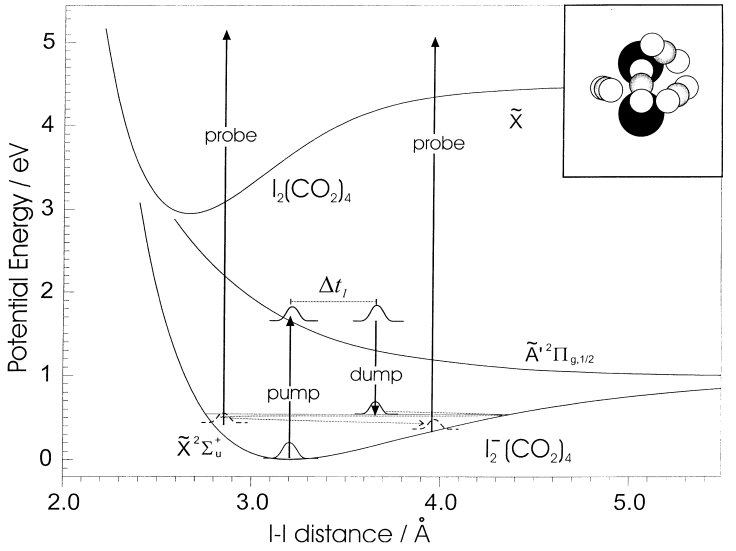

Fig. 1. Schematic of the SEP–FPES technique, including approximate potential curves for ground and excited state $I_2^-(CO_2)_4$, and ground state I_2. The anion potentials shown are simply those of I_2^- [19,21] shifted to lower energy by 0.429 eV, the measured stabilization energy of four CO_2 molecules [12]. Wavepackets drawn in a solid line are impacted by the pump and dump laser pulses which comprise the SEP process and are delayed by Δt_1 with respect to each other. The subsequent oscillation and relaxation of the excited wavepacket (dashed) is illustrated following the dashed arrow. Detachment by the probe pulse is shown for two arbitrary delay times, when the ground state wavepacket is located at the inner and outer turning points.

these effects are seen in the results presented here, in which we perform SEP–FPES on $I_2^-(CO_2)_4$ at a single excitation energy, 0.53 eV.

2. Experimental

A detailed description of the experimental apparatus [21,22], including the modifications necessary to incorporate the dump pulse [19], has been given elsewhere; only a brief summary is provided here. $I_2^-(CO_2)_n$ clusters are formed by passing a 1.8% mix of CO_2 in Ar at 20 psig over crystalline iodine. This mixture is supersonically expanded through a pulsed valve at 500 Hz and crossed with a 1 keV electron beam just downstream of the valve orifice. Anions formed in the expansion are injected into a Wiley–McLaren time-of-flight mass spectrometer [23] in which they separate temporally according to their mass. After passing through several differentially pumped chambers, clusters of the desired mass are intercepted at the focus of a magnetic bottle photoelectron spectrometer [24] by the pump, dump, and probe laser pulses. A reflectron mass analyzer downstream from the laser interaction region can be used to identify ionic photofragments created by either the pump pulse alone or by the combination of pump and dump pulses. Because of the high velocity of the ion beam (1.9 kV), the electron energy resolution in these studies is about 300 meV at 1.6 eV electron kinetic energy (eKE), and increases as approximately $(eKE)^{1/2}$; while the resolution can be improved considerably by pulsed deceleration of the ions, this was not done in the work reported here.

The pump, dump, and probe pulses are generated by a Clark-MXR regeneratively amplified Ti:sapphire laser system, which produces fundamental pulses at 795 nm (1.56 eV), 1 mJ, and 80 fs ($sech^2$) in time duration. About 40 μJ of this fundamental beam is used as the pump pulse; 500 μJ is used to pump a light conversion optical parametric amplifier (OPA) which produces the 1200-nm (1.03-eV), 50-μJ, 80-fs dump pulses. The remainder of the fundamental beam is frequency-tripled, yielding a 265-nm (4.68-eV), 20-μJ, 130-fs probe pulses. The time delays between pump, dump, and probe pulses are controlled by passing the pump and probe pulses through computer-controlled translation stages prior to collinear recombination of the three beams before entering the vacuum chamber. The pump–dump delay was fixed at 75 fs, and the dump–probe delay was varied during the course of the experiment. Above-threshold-detachment of I^- is used to determine the absolute zero-of-time within the spectrometer.

In order to normalize spectra at different pump–dump–probe delay times, a phase locked chopper alternately blocks and passes the dump pulse, and the ''dump-off'' spectra are dynamically subtracted from the ''dump-on'' spectra to create a difference spectrum. At each dump–probe delay, the pump–probe only spectra are also recorded, and are used to normalize difference spectra at different delay times to each other.

3. Results

Fig. 2 shows the probe-only, one-photon photoelectron spectrum of $I_2^-(CO_2)_4$. In this spectrum, which has been reported previously [12], the peak at 1 eV is from detachment to the $\tilde{X}$ state of neutral $I_2(CO_2)_4$, while the peak around 0.4 eV is due to unresolved detachment to the $\tilde{A}$ and $\tilde{A}'$ neutral states. The pump and dump pulses at 795 and 1200 nm create a wavepacket with excitation energy $h\nu_{pump} - h\nu_{dump} = 0.53$ eV. This wavepacket will have significant amplitude at the inner and outer turning points, and, as can be seen in Fig. 1, this will result in signal at higher and lower electron kinetic energies, respectively, than would result from photodetachment of $I_2^-(v=0)$. As a result we expect the signal due to SEP to occur in the boxed-in areas shown in Fig. 2.

Fig. 3a and b shows difference spectra (i.e., [pump + dump + probe] − [pump + probe]) at several dump–probe delay times. The positive signal above 1.5 eV and around 0.7 eV is from vibrationally excited I_2^- created by the pump and dump pulses. The origin of the depletion around 1.2 eV was discussed in our earlier work on bare I_2^- [19]. This is the region of the spectrum where signal from dissociation products on the repulsive $\tilde{A}'\ ^2\Pi_{g,1/2}$ state (see Fig. 1) is observed. Since part of the dissociating wavepacket created by the pump pulse is driven

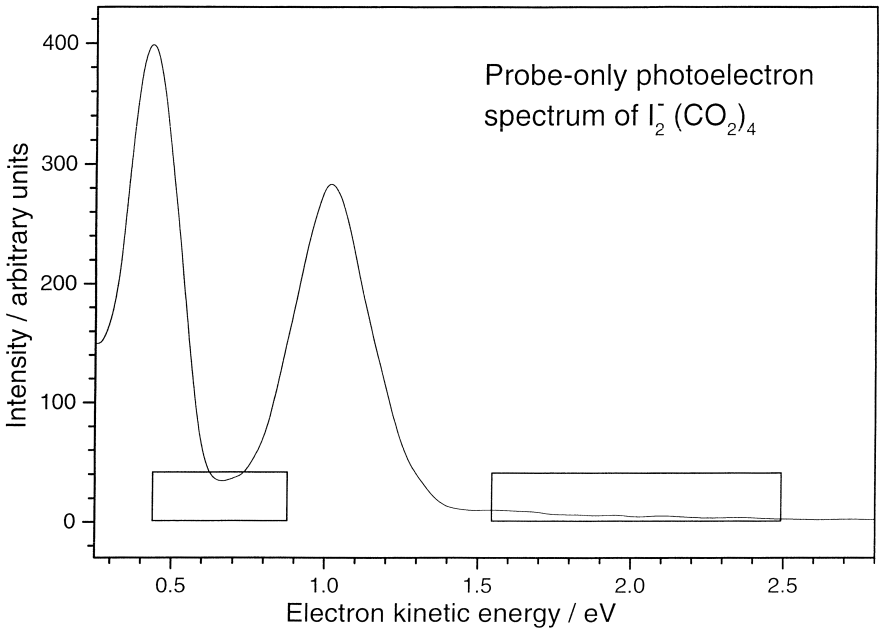

Fig. 2. Probe-only FPE Spectrum of $I_2^-(CO_2)_4$. The probe energy is 4.68 eV. Boxed areas represent regions where signals due to vibrationally excited $I_2^-(CO_2)_4$, which will be created by femtosecond SEP, are expected.

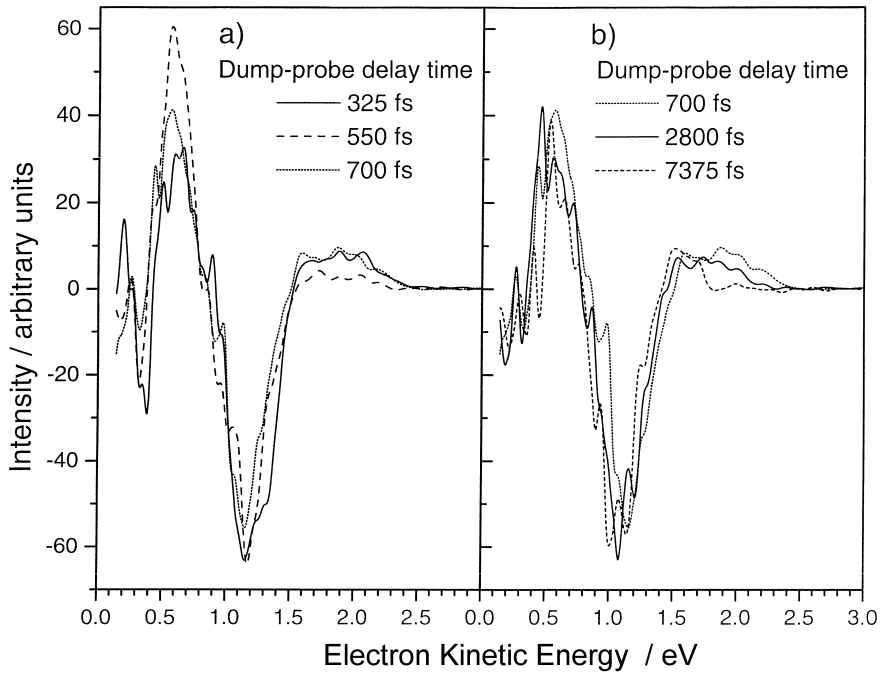

Fig. 3. FPE Spectra of $I_2^-(CO_2)_4$, with shot-to-shot background subtraction (Section 2) employed. Three early dump–probe delay times, representing the first oscillation of the wavepacket. Three dump–probe delays encompassing a time interval of several picoseconds. The high-eKE edge of the SEP signal shifts significantly to lower energy during this period.

back down to the $\tilde{X}$ state by the dump pulse, the dissociation yield is less when the dump pulse is on and depletion of the associated electron signal is observed.

The SEP-induced features in the spectra change with time and, in fact, exhibit oscillatory behavior at least at short times. Fig. 3a shows that the SEP-induced signal above 1.5 eV is maximal at 325 and 700 fs but considerably less at 550 fs, while the time-dependence of the signal at 0.7 eV is the reverse of that at high eKE. The time-dependence of the SEP-induced signal in these energy ranges is displayed more clearly in Fig. 4, which shows slices through the spectra at eKE values of 1.875 and 0.7 eV. Oscillations in the electron signal are evident, as is the fact the oscillations at the two electron energies are 180° out-of-phase. This phase lag is entirely consistent with our expectation that the signal at low and high eKE is from the outer and inner turning points, respectively, of the wavepacket. Note that the earliest maximum occurs in the 0.7 eV trace, as expected for stimulated emission of an outgoing (dissociating) wavepacket (see Fig. 1).

While the oscillations in Fig. 4 are similar to what was seen previously for bare I_2^-, there are two important differences. First, dephasing of the oscillations is more rapid in Fig. 4, occurring in about 3 ps rather than 7 ps for bare I_2^-. Second, while not entirely evident upon inspection of Fig. 4, the frequency of the oscillations is not constant with time, and increases from 0–3 ps. No such change was seen for bare I_2^-. A third difference is evident in the longer-time spectra shown in Fig. 3b: between 700 and 2800 fs the high-eKE edge of the spectrum shifts approximately 160 meV to lower energy, and between 2800 and 7375 fs the shift is an additional 330 meV. Such a shift was not observed in SEP–FPES experiments on the bare ion [19]. These three effects unique to $I_2^-(CO_2)_4$ are indicative of solvent interactions and will be addressed in the next section.

Fig. 5 shows photofragment mass spectra obtained using the reflectron assembly in the instrument with and without the dump pulse. The main fragment resulting from vibrational excitation of the parent cluster is $I_2^-(CO_2)$, seen only when the dump laser is on. Also present in both spectra are $I^-(CO_2)_2$ and

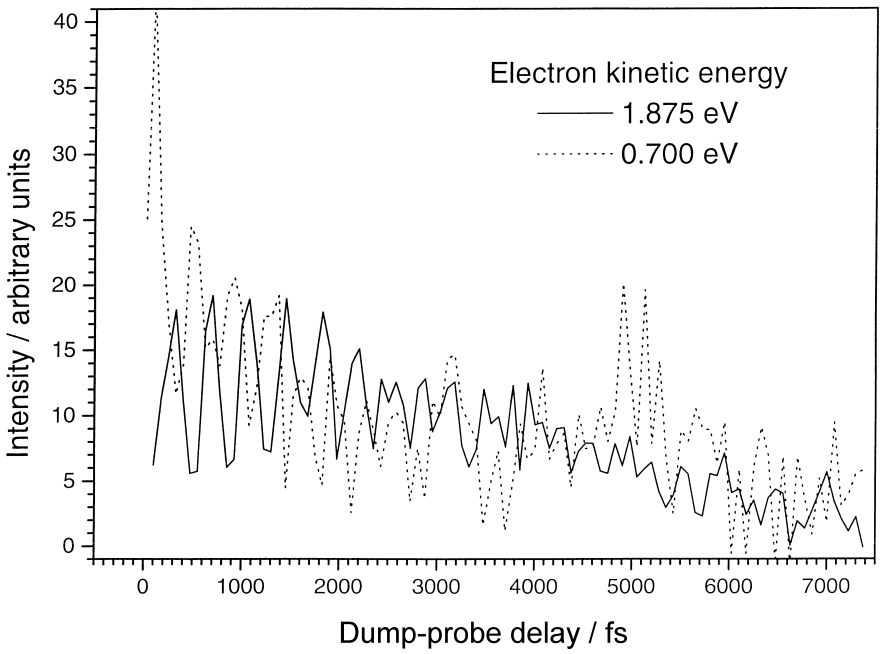

Fig. 4. Slices through the SEP signal at two values of electron kinetic energy. The oscillations at 1.875 eV monitor the vibrationally excited inner turning point of the potential; those at 0.700 eV are out of phase with the inner turning point and so must monitor the outer turning point. The oscillations dephase around 3 ps.

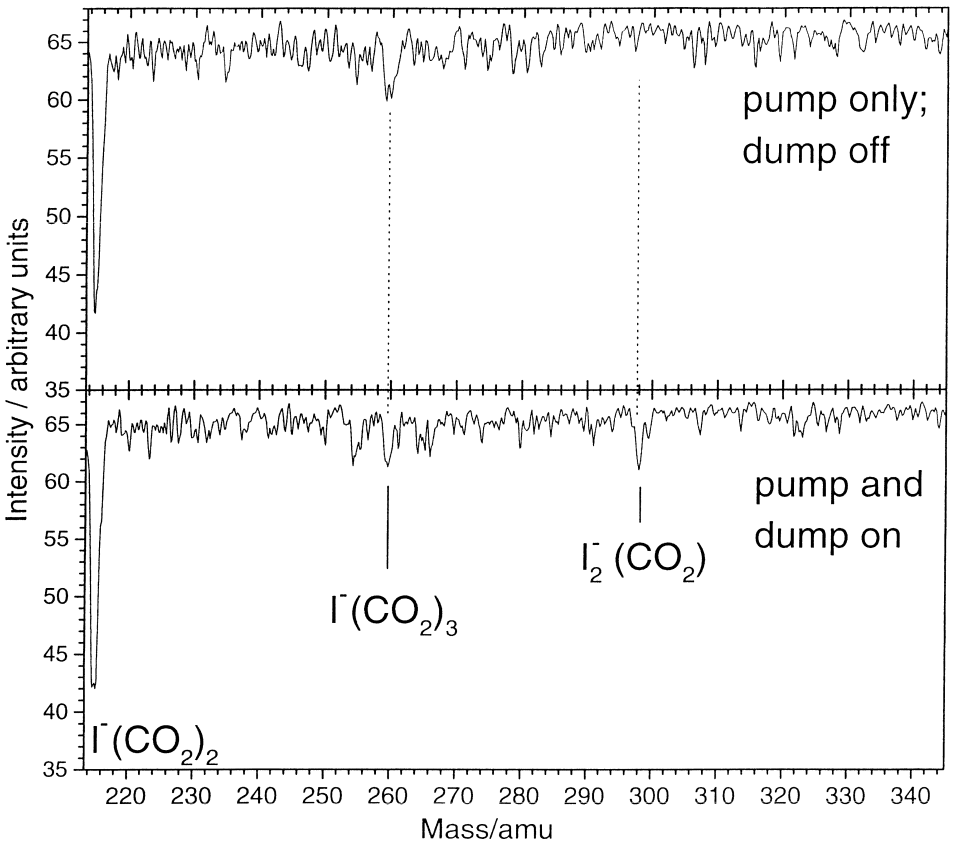

Fig. 5. Reflectron mass spectra of photofragments produced by pump pulse alone (upper spectrum) and by pump and dump pulses (lower). $I^-(CO_2)_n$ products ($n=2$ and 3), present in both spectra, are created on the $\tilde{A}'$ excited potential by the pump pulse alone. The $I_2^-(CO_2)$ fragment is created with the addition of the dump pulse, and represents the long-time evolution of the vibrationally excited state created by the SEP process.

$I^-(CO_2)_3$ photofragments which are created by the pump pulse alone.

4. Analysis and discussion

In this section we consider the solvent effects in the SEP–FPES spectra in more detail. The two most interesting effects are the increase in oscillation frequency with time and the shifting of the spectrum in the high eKE region toward lower eKE. Both of these effects reflect vibrational relaxation of the I_2^- chromophore. As the vibrating I_2^- loses energy, the frequency spacing between adjacent vibrational levels increases due to the anharmonicity of the I_2^- potential, and this spacing determines the frequency of the wavepacket oscillations. A similar effect was seen by Bargheer et al. [25] for I_2 in a Kr matrix excited by a femtosecond pulse to various vibrational energies within the $B\ ^3\Pi_{0u}$ bound state. In addition, as the I_2^- relaxes, the inner turning point for its vibrational wavefunction shifts to larger internuclear distances, thereby reducing the maximum electron kinetic energy.

4.1. Time-dependent wavepacket oscillation frequency

We first consider the oscillatory structure in the time-dependent photoelectron spectra. In order to assign the frequency of these oscillations, the oscillatory slice through 1.875 eV (at the inner turning

point) was fitted to the product of an exponential and a cosine function. The exponential serves to model the envelope of the data, while the cosine incorporates the oscillations. The function is given in Eq. (1); capital letters denote fitted parameters.

$$I(t) = A(B + e^{-(t-C)^2/D}) \cos[(E + F \times t)t + G] \quad (1)$$

A four-point running average was subtracted from the slice prior to fitting in order to remove low-frequency noise and offset. A fixed frequency cosine function did not fit the data, but a frequency linearly dependent on time afforded a good agreement.

The subtracted slice and the result of a nonlinear least-squares fit with Eq. (1) are shown in Fig. 6. The data was fitted up to 3325 fs, as indicated by the arrow. After this time, the oscillations have dephased, and the structure that remains is due to inherent noise. The important parameters to be extracted from the function are the frequency at $t=0$ (E) and the change in frequency with time (F). Converted to wavenumbers, these are 80 ± 1.5 cm^{-1} and 3.8 ± 0.5 cm^{-1}/ps. Thus over the approximate 3 ps of coherent motion, the measured frequency at the inner turning point increases from 80 to 91 cm^{-1}. We assign 80 cm^{-1} to be the energy interval between vibrational levels of the potential at 0.53 eV, and the increase in frequency to vibrational energy loss to the CO_2 molecules.

The initial frequency, 80 cm^{-1}, is significantly different from the value of 73.2 cm^{-1} which would result from bare I_2^- with the same excitation energy [19]. This shift is due to an inherent steepening of the anion potential due to solvent interaction. We have previously shown, using resonance impulsive stimulated Raman scattering (RISRS) probed by FPES, that the fundamental $I_2^-(CO_2)_4$ vibrational frequency (i.e., the energy spacing between the I_2^- $v=0$ and 1 levels) is blue shifted from that in bare I_2^- by 1.7 cm^{-1} [26]. This shift was attributed to attractive interactions between the iodine atoms and equatorial CO_2 molecules, with electron delocalization effects possibly playing a small part. The larger shift in the SEP experiments is caused by the same effects occurring higher in the potential well.

We next consider the increase in frequency with

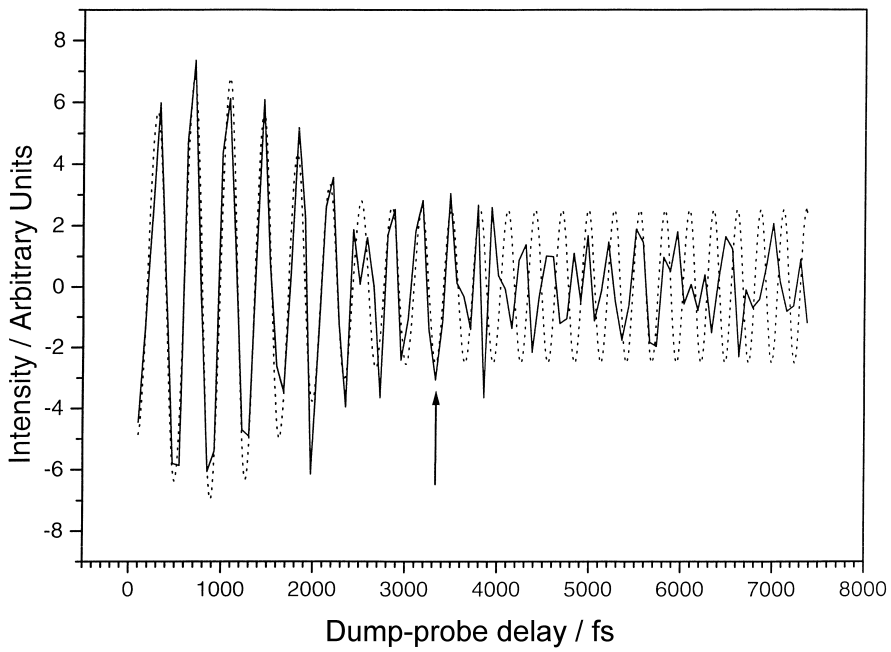

Fig. 6. Solid line: slice through 1.875 eV eKE, with four-point running average subtracted. Dashed line: results of a nonlinear least-squares fit to Eq. (1), performed from 0 to 3225 fs (arrow). Best-fit constants: $A=4.4\pm0.8$; $B=0.57\pm0.23$; $C=871\pm134$ fs; $D=9.9\times10^5\pm5.5\times10^5$ fs^2; $E=1.504\times10^{-2}\pm2.9\times10^{-4}$ rad fs^{-1}; $F=7.1\times10^{-7}\pm9\times10^{-8}$ rad fs^{-2}; $G=1.8\pm0.2$ rad.

time. In order to extract the amount of energy loss from the degree of frequency increase, we must assume a shape for the $I_2^-(CO_2)_4$ potential. In the following analysis, we assume that the cluster potential is identical to that of bare I_2^-. Given this assumption, we may use the dependence of the frequency of bare I_2^- on the amount of vibrational energy in order to estimate the energy transfer to solvent.

In the first 3 ps after the SEP wavepacket is created with 0.53 eV excitation energy, the frequency of oscillation of $I_2^-(CO_2)_4$ increases from 80 cm^{-1} to approximately 91 cm^{-1}. In bare I_2^- vibrationally excited by 0.53 eV, the vibrational frequency would be 73.2 cm^{-1}, and an increase of 11 cm^{-1} would correspond to a decrease in vibrational energy of 0.15 eV. Although the I_2^- potential clearly does not describe that of $I_2^-(CO_2)_4$, the slopes of the frequency–energy curve for the two systems are likely to be similar. Therefore, based on the fitted frequency shift, we estimate that $I_2^-(CO_2)_4$ loses 0.15 eV of vibrational energy in 3 ps.

4.2. Shifts in the photoelectron spectrum

We can also extract the vibrational energy loss by considering the shift in electron kinetic energy of the photoelectron spectra themselves, a useful procedure because it can be applied after 3 ps (i.e., after dephasing has occurred). Like the frequency analysis, this analysis also involves several approximations. The eKE shift itself is not easily quantifiable; the high-eKE portion of the spectrum is a relatively small positive signal immediately adjacent to the large negative signal of the depletion of the photodissociation products. If the high-eKE portion shifts significantly to lower eKE, it in effect ''falls into'' the depletion, where its magnitude cannot be easily monitored. Therefore, the high eKE edge of the SEP signal, rather than its peak, is the easiest part of the spectrum to track, although near the depletion (at long times) its measurement may be biased toward too-high energies. We assume that this high-eKE edge corresponds directly to the inner turning point of the anion potential. In addition, shapes for both the neutral and anion potentials must be assumed; here, again, we use those of the bare I_2^- and I_2, with the anion potential shifted to lower energy by 0.429 eV to account for its relative stabilization by the four CO_2 molecules [12]. With these assumptions, the energy shift can be determined by plotting the position of the high-eKE edge at each time delay. Using this information and the assumed potentials, the position of the inner turning point and thus the amount of vibrational excitation is extracted.

The resulting plot of vibrational energy versus time is shown in Fig. 7. At early times, fewer data points are plotted because the oscillations in intensity (due to the wavepacket coherence) make it difficult to determine the high-eKE edge for each recorded delay time. A single exponential fit to the calculated vibrational energies, also shown in Fig. 7, will be used to examine the rate of energy loss as determined by the photoelectron spectrum shift. The time constant of decay is 4440 ± 880 fs, and the amount of energy at $t=0$ is 0.58 eV. This is somewhat greater than the known value of 0.53 eV; the discrepancy is well within our spectral resolution, and may also be due to the approximate nature of the potentials used.

At dump–probe delay times of ≤ 3000 fs, the vibrational energy loss from the shifts in the spectra can be directly compared to the loss calculated by changes in the oscillation frequency. We find somewhat larger losses from the spectral shifts, i.e., 0.24 eV at 3000 fs vs. 0.15 eV determined from the change in frequency. This difference may reflect difficulties in choosing the exact eKE corresponding to the high energy edge of the photoelectron spectrum, since the shape of the spectrum at high eKE changes with time (see Fig. 3b). In any case, the two methods demonstrate qualitatively similar vibrational relaxation dynamics.

At times longer than 3 ps the oscillations have dephased. We cannot perform the frequency analysis past this point, and must use the shift of the spectra to estimate further energy losses. At 7000 fs after the dump pulse, the exponential fit to the spectral shift indicates that 0.38 eV of energy has been dissipated to the solvent at this time. At longer times, the spectral shift cannot be measured accurately because of overlap between the high energy signal from the inner turning point and the energy region where depletion occurs (see Fig. 3).

The energy lost through vibrational relaxation of

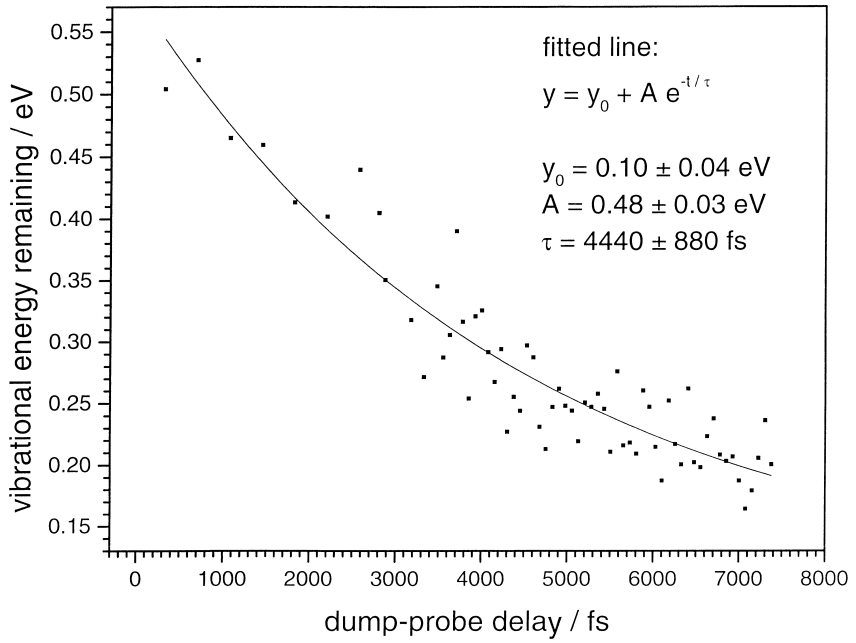

Fig. 7. Vibrational energy remaining in the I_2^- moiety within the cluster, determined by the high-energy edge of the photoelectron spectra. The line is a least-squares fit of the data with a single exponential decay, whose parameters are given.

the I_2^- is taken up by the solvent molecules and is ultimately lost through evaporation of solvent molecules from the cluster. The reflectron mass spectra in Fig. 6 measure the product mass distribution after several microseconds have elapsed and show that the vibrationally excited cluster eventually loses three solvent molecules, leaving $I_2^-(CO_2)$ as the stable product. However, no solvent evaporation occurs before 7 ps; if it did, the electron affinity of the cluster would drop significantly (i.e., ~0.1 eV per solvent molecule [12]) and we would see signal growing in at high eKE. No such effect is observed. Thus, there is a substantial delay between the vibrational relaxation of the I_2^- and evaporation of solvent molecules, consistent with our previous study of the photodissociation of $I_2^-(CO_2)_n$ clusters [12], in which the average vibrational level of recombined I_2^- changed much more quickly than the average number of solvent molecules surrounding the recombined I_2^-. This was found to be true especially for clusters which recombined on the ground state with fewer than 11 CO_2 molecules remaining.

4.3. Dephasing of oscillations

The oscillations in the photoelectron intensity for vibrationally excited $I_2^-(CO_2)_4$ dephase by about 3 ps. This dephasing is caused by a combination of the anharmonicity of the I_2^- potential and the effects of the CO_2 solvent molecules on the coherence of the wavepacket created by SEP. Bare I_2^- excited via SEP to a similar energy region dephases after about 7 ps; since dephasing in the bare ion is due solely to the potential anharmonicity, the early dephasing in the cluster must be due to solvent–solute interactions that over several vibrational periods irreversibly destroy the coherence of the wavepacket.

5. Conclusions

We have applied femtosecond stimulated emission pumping to study the vibrational relaxation of excited I_2^- within a cluster of four CO_2 molecules. The use of SEP to directly produce the vibrational

superposition allows ground state vibrational relaxation to be monitored independent of the caging and solvent loss inherent to photodissociation-based techniques. In this manner, the initial vibrational energy of the chromophore is known and tunable, wavepacket coherence is maintained during the first several vibrational periods, and the rates of dephasing and of energy loss to the solvent can be examined as a function of solvent number, solvent type, and initial excitation.

When monitored by FPES, the amount of energy transfer can be determined either by the change in oscillation frequency (while the wavepacket is still coherent) and/or by the shift in the photoelectron spectrum. The vibrational frequency of the potential of $I_2^-(CO_2)_4$ at 0.53 eV excitation energy is significantly greater than that of bare I_2^-. Vibrational energy loss by the I_2^- occurs on a time scale of 4.4 ps, while solvent evaporation occurs much more slowly. Future work will proceed in three directions. Within a single cluster size, we will examine several excitation energies in order to probe the energy dependence of the vibrational relaxation rate, as well as develop more accurate potentials for the clusters. In addition, we will vary the cluster size to examine the effect of additional solvent molecules on relaxation rates, and we will study vibrational relaxation in different solvent clusters, in order to explore the effects on energy redistribution of different solvent–solute interactions.

Acknowledgements

This research was supported by the National Science Foundation under Grant No. CHE-9710243 and by the Defense University Research Instrumentation Program under Grant No. F49620-95-0078. C.F. acknowledges post-doctoral support from the Deutsche Akademie der Naturforscher Leopoldina (BMBF-LPD 9801-6). A.V.D. is a National Science Foundation predoctoral fellow. M.E. and D.M.N. thank the France–Berkeley Fund for financial support.

References

[1] R.M. Stratt, M. Maroncelli, J. Phys. Chem. 100 (1996) 12981.
[2] A.E. Johnson, N.E. Levinger, P.F. Barbara, J. Phys. Chem. 96 (1992) 7841.
[3] J.C. Alfano, Y. Kimura, P.K. Walhout, P.F. Barbara, Chem. Phys. 175 (1993) 147.
[4] P.K. Walhout, J.C. Alfano, K.A.M. Thakur, P.F. Barbara, J. Phys. Chem. 99 (1995) 7568.
[5] J.M. Papanikolas, J.R. Gord, N.E. Levinger, D. Ray, V. Vorsa, W.C. Lineberger, J. Phys. Chem. 95 (1991) 8028.
[6] J.M. Papanikolas, V. Vorsa, M.E. Nadal, P.J. Campagnola, H.K. Buchenau, W.C. Lineberger, J. Chem. Phys. 99 (1993) 8733.
[7] V. Vorsa, S. Nandi, P.J. Campagnola, M. Larsson, W.C. Lineberger, J. Chem. Phys. 106 (1997) 1402.
[8] A. Sanov, S. Nandi, W.C. Lineberger, J. Chem. Phys. 108 (1998) 5155.
[9] A. Sanov, T. Sanford, S. Nandi, W.C. Lineberger, J. Chem. Phys. 111 (1999) 664.
[10] B.J. Greenblatt, M.T. Zanni, D.M. Neumark, Science 276 (1997) 1675.
[11] B.J. Greenblatt, M.T. Zanni, D.M. Neumark, J. Chem. Phys. 111 (1999) 10566.
[12] B.J. Greenblatt, M.T. Zanni, D.M. Neumark, J. Chem. Phys. 112 (2000) 601.
[13] J. Faeder, N. Delaney, P.E. Maslen, R. Parson, Chem. Phys. Lett. 270 (1997) 196.
[14] N. Delaney, J. Faeder, P.E. Maslen, R. Parson, J. Phys. Chem. A 101 (1997) 8148.
[15] J. Faeder, N. Delaney, P.E. Maslen, R. Parson, Chem. Phys. 239 (1998) 525.
[16] J. Faeder, R. Parson, J. Chem. Phys. 108 (1998) 3909.
[17] V.S. Batista, D.F. Coker, J. Chem. Phys. 106 (1997) 7102.
[18] C.J. Margulis, D.F. Coker, J. Chem. Phys. 110 (1999) 5677.
[19] M.T. Zanni, A.V. Davis, C. Frischkorn, M. Elhanine, D.M. Neumark, J. Chem. Phys. 112 (2000) 8847.
[20] N. Delaney, J. Faeder, R. Parson, private communication.
[21] M.T. Zanni, V.S. Batista, B.J. Greenblatt, W.H. Miller, D.M. Neumark, J. Chem. Phys. 110 (1998) 3748.
[22] B.J. Greenblatt, M.T. Zanni, D.M. Neumark, Faraday Discuss. 108 (1998) 101.
[23] W.C. Wiley, I.H. McLaren, Rev. Sci. Instrum. 26 (1955) 1150.
[24] O. Cheshnovsky, S.H. Yang, C.L. Pettiette, M.J. Craycraft, R.E. Smalley, Rev. Sci. Instrum. 58 (1987) 2131.
[25] M. Bargheer, P. Dietrich, K. Donovang, N. Schwentner, J. Chem. Phys. 111 (1999) 8556.
[26] M.T. Zanni, B.J. Greenblatt, D.M. Neumark, J. Chem. Phys. 109 (1998) 9648.